Microtubule Targeting of Substrate Contacts Promotes Their Relaxation and Dissociation✪

Irina Kaverina, Olga Krylyshkina, and J. Victor Small

Institute of Molecular Biology, Austrian Academy of Sciences, A-5020 Salzburg, Austria

Abstract. We recently showed that substrate contact sites in living fibroblasts are specifically targeted by microtubules (Kaverina, I., K. Rottner, and J.V. Small. 1998. *J. Cell Biol.* 142:181–190). Evidence is now provided that microtubule contact targeting plays a role in the modulation of substrate contact dynamics. The results are derived from spreading and polarized goldfish fibroblasts in which microtubules and contact sites were simultaneously visualized using proteins conjugated with Cy-3, rhodamine, or green fluorescent protein.

For cells allowed to spread in the presence of nocodazole the turnover of contacts was retarded, as compared with controls and adhesions that were retained under the cell body were dissociated after microtubule reassembly. In polarized cells, small focal complexes were found at the protruding cell front and larger adhesions, corresponding to focal adhesions, at the retracting flanks and rear. At retracting edges, multiple microtubule contact targeting preceded contact release and cell edge retraction. The same effect could be observed in spread cells, in which microtubules were allowed to reassemble after local disassembly by the application of nocodazole to one cell edge. At the protruding front of polarized cells, focal complexes were also targeted and as a result remained either unchanged in size or, more rarely, were disassembled. Conversely, when contact targeting at the cell front was prevented by freezing microtubule growth with 20 nM taxol and protrusion stimulated by the injection of constitutively active Rac, peripheral focal complexes became abnormally enlarged. We further found that the local application of inhibitors of myosin contractility to cell edges bearing focal adhesions induced the same contact dissociation and edge retraction as observed after microtubule targeting.

Our data are consistent with a mechanism whereby microtubules deliver localized doses of relaxing signals to contact sites to retard or reverse their development. We propose that it is via this route that microtubules exert their well-established control on cell polarity.

Key words: cytoskeleton • signaling • contractility • cell polarity • actin

THE processes of polarization and cell motility of substrate-bound cells may be viewed as a competition between the motile compartment of the actin cytoskeleton, comprising lamellipodia and filopodia, and the anchorage compartment, embracing the stress fiber bundles and focal adhesions. For cell translocation, these compartments must be regionally segregated and this state requires an intact microtubule cytoskeleton (Vasiliev and Gelfand, 1976). Mounting evidence now indicates that the route by which microtubules exert their control on actin cytoskeleton organization and polarity impinges on the Rho-dependent pathways leading to substrate contact formation. Such a link was first indicated by the findings that microtubule disruption leads to the activation of Rho, with the consequent induction and enlargement of focal adhesions (Danowski, 1989; Bershadsky et al., 1996; Enomoto, 1996). Further studies have provided evidence for a direct spatial interaction between microtubules and adhesion sites (Kaverina et al., 1998). Thus, by simultaneously recording the dynamics of microtubules and substrate contacts in living fibroblasts, it was demonstrated that microtubule growth towards the cell periphery is associated with a specific targeting of substrate contact sites. Since substrate contacts were observed to confer stability against depolymerization to targeting microtubules and could also act as sites of microtubule nucleation during recovery from nocodazole, it was concluded that microtubule contact interfacing represents a functionally relevant process (Kaverina et al., 1998).

What influence, then, do microtubules have on substrate contact dynamics? In this study we sought to clarify how

✪The online version of this article contains supplemental material.

Address correspondence to J. Victor Small, Austrian Academy of Sciences, Institute of Molecular Biology, Department of Cell Biology, Billrothstrasse 11, Salzburg A-5020, Austria. Tel.: (43) 662-63961-11. Fax: (43) 662-63961-40. E-mail: jvsmall@imb.oeaw.ac.at

these targeting interactions may explain the control exerted by microtubules on cell polarity. Our findings are consistent with a mechanism whereby the turnover of contact sites is modulated by the delivery of relaxing impulses to contacts in a precise, site-specific manner via microtubule targeting. We propose that differential effects on contact sites, necessary to effect cell polarization, are achieved by the microtubule dependent delivery of relaxation signals at different stages of contact maturation.

Materials and Methods

Cells

Goldfish fin fibroblasts (line CAR, no. CCL71; American Type Culture Collection) were maintained in basal Eagle medium with Hanks' BSS and nonessential amino acids and with 15% fetal calf serum at 25°C. For experiments, cells were plated onto coverslips coated with human serum fibronectin (Boehringer Mannheim GmbH) for at least 48 h. Fibronectin was coated onto polylysine-treated coverslips by incubation on a drop of 50 μg/ml fibronectin in PBS at 4°C overnight; after rinsing in PBS these coverslips were used without drying. Fibronectin was stored as a stock solution in 2 M urea at 4°C. For polylysine coating, coverslips were incubated on a drop of aqueous 100 μg/ml polylysine for 30 min at room temperature (RT)[1], rinsed with water, dried, and UV sterilized.

Microinjection

Injections were performed with sterile Femtotips (Eppendorf) held in a Leitz Micromanipulator with a pressure supply from an Eppendorf Microinjector 5242. Cells were injected with a continuous outflow mode from the needle under a constant pressure of between 20 and 40 hPa. For local application of drugs, performed with the same system, a constant pressure of 50–100 hPa was used.

Proteins for Microinjection and Drugs

Tetramethyl rhodamine (5-TAMRA; Molecular Probes) conjugated vinculin from turkey gizzard was kindly provided by Mr. K. Rottner and Dr. M. Gimona (Institute of Molecular Biology, Salzburg, Austria). Small aliquots in 2 mg sucrose/mg protein were stored at −70°C. Before use, the fluorescent vinculin was dialyzed against 2 mM Tris-Acetate, pH 7.0, 50 mM KCl, 0.1 mM DTE, and used at a concentration of ~1 mg/ml. Cy3-conjugated tubulin was kindly provided by J. Peloquin and Dr. G. Borisy (University of Wisconsin, Madison, WI). It was stored at a concentration of 10 mg/ml in aliquots at −70°C. Rhodamine-conjugated rat tubulin was kindly provided by Drs. R. Tournebize and T. Hyman (EMBL, Heidelberg) and stored at −70°C in 5-μl aliquots (~20 mg/ml) in BRB80 buffer (80 mM Pipes, pH 6.8, 1 mM $MgCl_2$, and 1 mM EGTA). For microinjection, rhodamine tubulin aliquots were diluted 1:3 with Tris-acetate injection buffer (2 mM Tris-acetate, pH 7.0, 50 mM KCl, and 0.1 mM DTE) and used on the same day. For coinjections, tubulin and vinculin were mixed after separate centrifugation for 10 or more min at 18,000 *g* in a proportion of 1:4 and used immediately.

Recombinant L61Rac was kindly provided by K. Rottner (using a construct originally provided by Professor A. Hall), dialyzed into 50 mM Tris (pH 7.5), 150 mM NaCl, 5 mM $MgCl_2$, and 1 mM DTE for microinjection (Nobes and Hall, 1995), and injected at a concentration of 2 mg/ml.

For local application through a microneedle, drugs were dissolved in microinjection buffer (2 mM Tris-Acetate, pH 7.0, 50 mM KCl, and rhodamine dextran as a marker): the inhibitor of myosin light chain kinase, ML-7 (Alexis Corporation) was used at a concentration of 2 mM; the actomyosin inhibitor 2,3-butanedione 2-monoxime (BDM) was used as a saturated solution (~500 mM); and nocodazole (Sigma Chemical Co.) was used at a concentration of 160 μM. Complete depolymerization of microtubules for spreading experiments was achieved using a concentration of 2.5 μg/ml. Cells were preincubated with nocodazole for 1–3 h and replated in the presence of the drug. Nocodazole was stored as a 16-mM stock solution in DMSO. A low concentration (20 nM) of taxol (paclitaxel; Sigma Chemical Co.) was used for suppression of microtubule dynamics. Taxol was stored as an 10 mM stock solution in DMSO. The inhibitor of p160ROCK, Y27632 (Uehata et al., 1997), was added to culture medium at a concentration of 100 μM, obtained by dilution from a 10-mM stock solution in DMSO.

Transfections

For coexpression of GFP-fused proteins, mouse β 3 tubulin in a pEGFP-C2 vector and human zyxin in a pEGFP-N1 vector were used. Both probes were kindly provided by Professor J. Wehland and coworkers (BGF, Braunschweig, Germany). Subconfluent monolayer cultures on 30-mm petri dishes were used for transfection. For each dish, the transfection mixture was prepared as follows: 1 μg of EGFP-zyxin DNA and 2 μg of EGFP-β-tubulin DNA and 14 μl of Superfect lipofection agent (Qiagen) were mixed in 400 μl of serum-free medium. After 30 min incubation at RT a further 1.2 ml of medium containing 5% serum was added. Cells were incubated in this mixture for 4 h at 25°C and the medium then replaced by normal medium containing 15% serum. After 24 h, cells were replated at a dilution of 1:15 onto coverslips for microscopy (see Cells).

The EGFP-zyxin expressing stable cell line was produced by transfection as above using 3 μg EGFP-zyxin DNA, followed by selection in 1 mg/ml G418 (GIBCO)-containing medium. Positive clones were identified in the fluorescence microscope and maintained in 0.4 mg/ml G418-containing medium.

Video Microscopy

Cells were injected and observed in an open chamber at RT on an inverted microscope (Axiovert 135TV; Zeiss) equipped for epifluorescence and phase contrast microscopy. Injections were performed at an objective magnification of 40× (NA 1.3 Plan Neofluar) and video microscopy with a 100×/NA 1.4 Plan-Apochromat with or without 1.6 optovar intermediate magnification. Filters blocking wavelengths below 590 nm were used for phase contrast illumination in order to avoid excitation of the fluorescent probe. Tungsten lamps (100 W) were used for both transmitted and epi-illumination. Data were acquired with a back-illuminated, cooled CCD camera from Princeton Research Instruments driven by IPLabs software (both from Visitron Systems) and stored as 16-bit digital images. The microscope was additionally equipped with shutters (Optilas GmbH) driven through a homemade interface to allow separate recordings of video sequences in phase contrast and fluorescence channels. Times between frames were 27 or 37 s. These time intervals are longer than used in the previous study (17 and 22 s in Kaverina et al., 1998), but were chosen so as to allow the recording of video sequences (50–100 frames) long enough to observe substrate contact turnover. Under these compromise conditions, not all targeting events would have been recorded. The video sequences were analyzed and processed on a Macintosh Power PC 7100/80 using IPLabs (Visitron Systems) and Adobe Photoshop 2.5.1 (Adobe Systems, Inc.) software.

Fluorescence Microscopy

For phalloidin stainings, cells were fixed for 10 min in 3% paraformaldehyde in cytoskeleton buffer (CB: 10 mM MES, 150 mM NaCl, 5 mM EGTA, 5 mM glucose, and 5 mM $MgCl_2$, pH 6.1) and extracted for 1 min in 0.25% Triton X-100 in the same buffer. Cy3-Phalloidin was a kind gift of Professor H. Faulstich (Max-Plank Institute, Heidelberg, Germany) and was used at a concentration of 0.2 μg/ml for 30 min at RT. Pictures of cells that were fixed and stained on the microscope were taken in 100 mM DTE in CB to avoid photobleaching.

Quantitative Analysis

For calculation of targeting frequency, 20-μm-wide regions of retracting and protruding edges of the same cells were compared.

Contacts within 5 μm of the cell edge were analyzed, and the number of targeting events for each contact in a time period of 15 min recorded. For comparison of the size of focal adhesions contact length was measured using the IPLabs Measure Length tool. Focal contact turnover in spreading cells was determined by following the fate of contacts newly formed at 15 min after a further 15-min period. All calculations and statistics were performed using KaleidaGraf version 2.3.1. (Synergy Software, Inc.).

1. *Abbreviations used in this paper:* BDM, 2,3-butanedione 2-monoxime; RT, room temperature.

Online Supplemental Material

The online version of this article includes videos that accompany several of the figures presented here. The video number, related figure, and URL are listed below.

Video 1: Fig. 1. http://www.jcb.org/cgi/content/full/146/5/1033/F1/DC1

Video 2: Fig. 3, A–C; Video 3: Fig. 3, D–F. http://www.jcb.org/cgi/content/full/146/5/1033/F3/DC1

Videos 4 and 5: Fig. 4, A–C, http://www.jcb.org/cgi/content/full/146/5/1033/F4/DC1

Video 6: Fig. 5 and Fig. 7 A; Video 7: Fig. 5 C. http://www.jcb.org/cgi/content/full/146/5/1033/F5/DC1

Video 8: Fig. 6. http://www.jcb.org/cgi/content/full/146/5/1033/F6/DC1

Video 9: Fig. 7 A. http://www.jcb.org/cgi/content/full/146/5/1033/F7/DC1

Video 10: Fig. 8. http://www.jcb.org/cgi/content/full/146/5/1033/F8/DC1

Results

Substrate Contact Turnover during Cell Spreading Is Potentiated by Microtubules

The spreading of a cell, when freshly plated onto a substrate may be likened to a state of unpolarized locomotion, in that protrusive activity occurs in all radial directions. Since freshly plated cells are more or less impossible to inject with fluorescent probes, we used goldfish fibroblasts (CAR cells) that had been stably transfected with EGFP-zyxin to follow contact dynamics during the spreading process.

Fig. 1 shows typical examples of the contact dynamics of spreading cells in which the microtubule system was either intact (Fig. 1 A), or disassembled by treatment before and during plating with nocodazole (Fig. 1 B). For comparison, video frames are shown for the same times after plating. The first, evident difference is the greater rate of spreading in the presence of an intact microtubule cytoskeleton; after 30 min, the total spread area of the cell in A was almost twice that achieved without microtubules (B). A second, notable difference was seen in the rate of turnover of the formed contact sites. This is best illustrated by referring to the contact sites marked with arrowheads for each of the series shown in Fig. 1. In A, the two marked contacts formed at the cell periphery at time 10′00″ after plating were no longer existent at 30′48″, having been superceded by new contacts formed under the advancing cell front. The same turnover of contacts was not seen in the presence of nocodazole. Instead, contacts formed at an early stage of spreading remained unchanged or elongated outwards (Fig. 1 B, arrowheads). Analysis of contact fate was made in 9 cells by counting the number of contacts that disappeared between 15 and 30 min of spreading. In control cells, 75% of a total of 91 contacts (4 cells) disappeared during this period, whereas only 22% of a total of 99 contacts (5 cells) disappeared in cells spreading in nocodazole.

An influence of microtubules on substrate contact turnover could also be observed during the reassembly of microtubules in cells that had first been allowed to spread to their maximum extent in the presence of nocodazole. In this case (Fig. 2) cells were used that had been transiently transfected with both EGFP-zyxin and EGFP-tubulin. As seen in Fig. 2, the recovery of the microtubule network was associated with the disassembly of a large proportion of contacts in the perinuclear region of the cell. Out of 61 nonperipheral contacts, 29 disappeared during microtubule recovery and 32 were retained, but even these became smaller or less intense. Video sequences from a further 3 cells showed similar results.

Elimination of Targeting Leads to Contact Growth

Since the active growth of microtubules was essential for targeting to occur, we modified microtubule growth kinetics to establish how this affected contact dynamics. Microtubules were first stabilized by brief treatment with taxol (20 μM, 30 min) and then, still in the presence of taxol, selected cells were injected with constitutively active

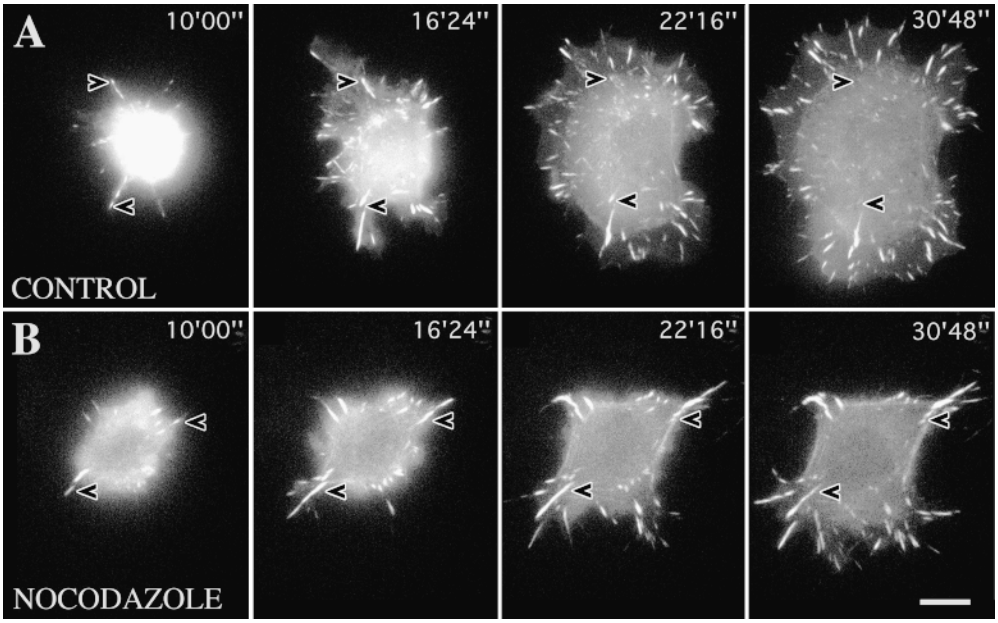

Figure 1. Substrate contact turnover during cell spreading is potentiated by microtubules. A: Video sequence of a spreading fish fibroblast transfected with EGFP-zyxin. (B) As in A but for a cell pretreated with and replated in the presence of 2.5 μg/ml nocodazole. Arrowheads indicate the position of representative contacts throughout the two sequences. Times are given in minutes and seconds. Bar, 10 μm. Video available at http://www.jcb.org/cgi/content/full/146/5/1033/F1/DC1

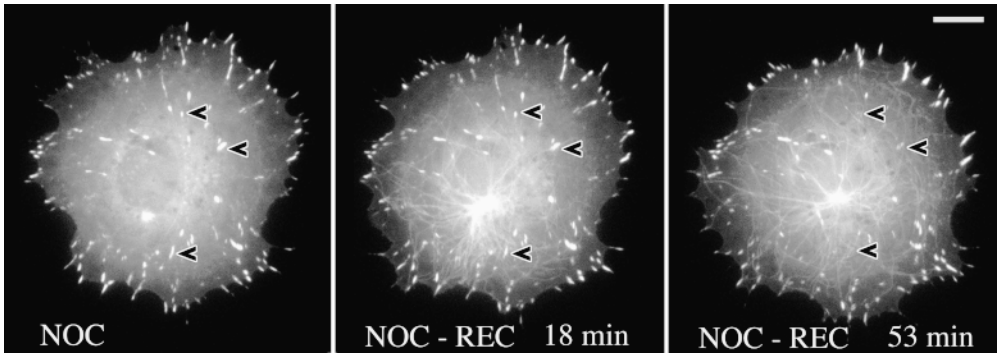

Figure 2. Focal adhesions are dissociated during recovery from nocodazole. Control image shows fish fibroblast cotransfected with EGFP-tubulin and EGFP-zyxin pretreated with and replated in 2.5 μg/ml nocodazole (NOC) for 1 h. Subsequent frames show recovery after nocodazole washout. Time is given in minutes and seconds. Arrowheads indicate some of the adhesion sites that were dissociated during microtubule reassembly. Bar, 10 μm.

L61Rac to induce the protrusion of lamellipodia and membrane ruffling. Microtubules and contacts were labeled in this case by the preinjection of cells (before taxol) with rhodamine-conjugated tubulin and vinculin. An example of such an experiment is shown in Fig. 3. At the time of Rac injection (Fig. 3 A; 0′00″), microtubules extended to the cell periphery but were no longer dynamic, according to the video analysis.

Rac injection induced an advance of the cell edge as well as active rearward cytoplasmic flow and ruffling activity. The combination of the block in microtubule polymerization and the centripetal flow, sweeping microtubules rearwards (Waterman-Storer and Salmon, 1998), created a microtubule-free border behind the lamellipodium. In this region, contact sites that were only just visible at time 0′00″ (white arrowheads in A) had become enlarged and elongated at the end of the sequence (Fig. 3 C; 28′14″). Notably, one peripheral contact (indicated by hollow arrow) that had remained associated with the end of a microtubule throughout did not increase in size.

Measurements of 10 cells made 1 h after injection with L61Rac, 5 in the absence and 5 in the presence of taxol, revealed an average length of peripheral contacts, formed after Rac injection, of 0.67 ± 0.07 μm for the control set (total 472 contacts) and 1.29 ± 0.12 μm for the taxol-treated cells (total 344 contacts). An example of a control cell injected with L61Rac is shown in Fig. 3, D–F, with a comparison in the inset (in F) of the peripheral contacts in C (taxol) at the same magnification.

Rho-kinase Independent Contact Sites Are also Targeted by Microtubules

In a parallel study on Swiss 3T3 cells (Rottner et al., 1999), it has been shown that the Rho kinase inhibitor, Y27632 (Uehata et al., 1997), causes the dissolution of Rho-dependent focal adhesions, but not of Rac-dependent peripheral "focal complexes" (Nobes and Hall, 1995) that are associated with lamellipodium protrusion and membrane ruffling. As in Swiss 3T3 cells (Rottner et al., 1999) and HeLa cells (Uehata et al., 1997), similar Rho-kinase independent focal complexes were found in CAR cells. Since many of these were elongated and associated with filopodia it is likely that their formation is not only dependent on Rac but also on Cdc42.

Analysis of a total of 14 cells treated with the Rho-kinase inhibitor showed that focal complexes were also targeted by microtubules. For these experiments, cells were doubly transfected with EGFP-tubulin and EGFP-zyxin. In the example shown in Fig. 4, the cell was fixed after the video sequence and stained with phalloidin (Fig. 4 C) to confirm that the concentration of Y27632 used (100 μM) had caused the disassembly of stress fiber bundles. As shown in the video sequence (Fig. 4 D), one contact (arrowhead) that first appeared at 17′24″ was targeted between 45′09″ and 45′46″ and had then dissociated 10 min later (55′38″). Additional, new contacts were formed as the cell edge protruded beyond this contact site and these were also targeted by microtubules (arrows at 64′53″).

Repetitive Targeting of Peripheral Focal Adhesions Precedes Cell Edge Retraction

During cell motility, the trailing parts of a cell develop strong contacts with the substrate (e.g., Chen, 1981) and must be retracted to support the locomotory efforts of the cell front. It was therefore pertinent to analyze targeting activities in retracting regions, carried out in this case with fibroblasts coinjected with fluorescent tubulin and vinculin.

An example of a moving cell is shown in Fig. 5 in which a lateral flank was retracted, in concert with the protrusion of the anterior lamellipodium. The video sequences revealed that the contact targeting frequency in the trailing flank was several fold higher than in the protruding front. 10 peripheral contacts between the two asterisks shown in A were all multiply targeted by microtubules. The number of targeting events in total were 57, amounting to an average of 5.7 targeting interactions for each contact. The sequence of events for one of the contacts is shown in Fig. 5 C. This contact, indicated at time 0′0″ with an open arrow, was targeted a total of 6 times, shown in the following 6 frames, and was retracted inwards after time 7′42″, along with the rest of the cell edge. The frequency of contact targeting in the protruding cell front during the same sequence was 0.75, that is eightfold less than at the retracting flank. For two other cells, corresponding targeting frequencies at retracting, versus protruding edges were 4.1 versus 0.28 (cell 2) and 4.3 versus 0.81 (cell 3).

To further assess the consequences of contact targeting,

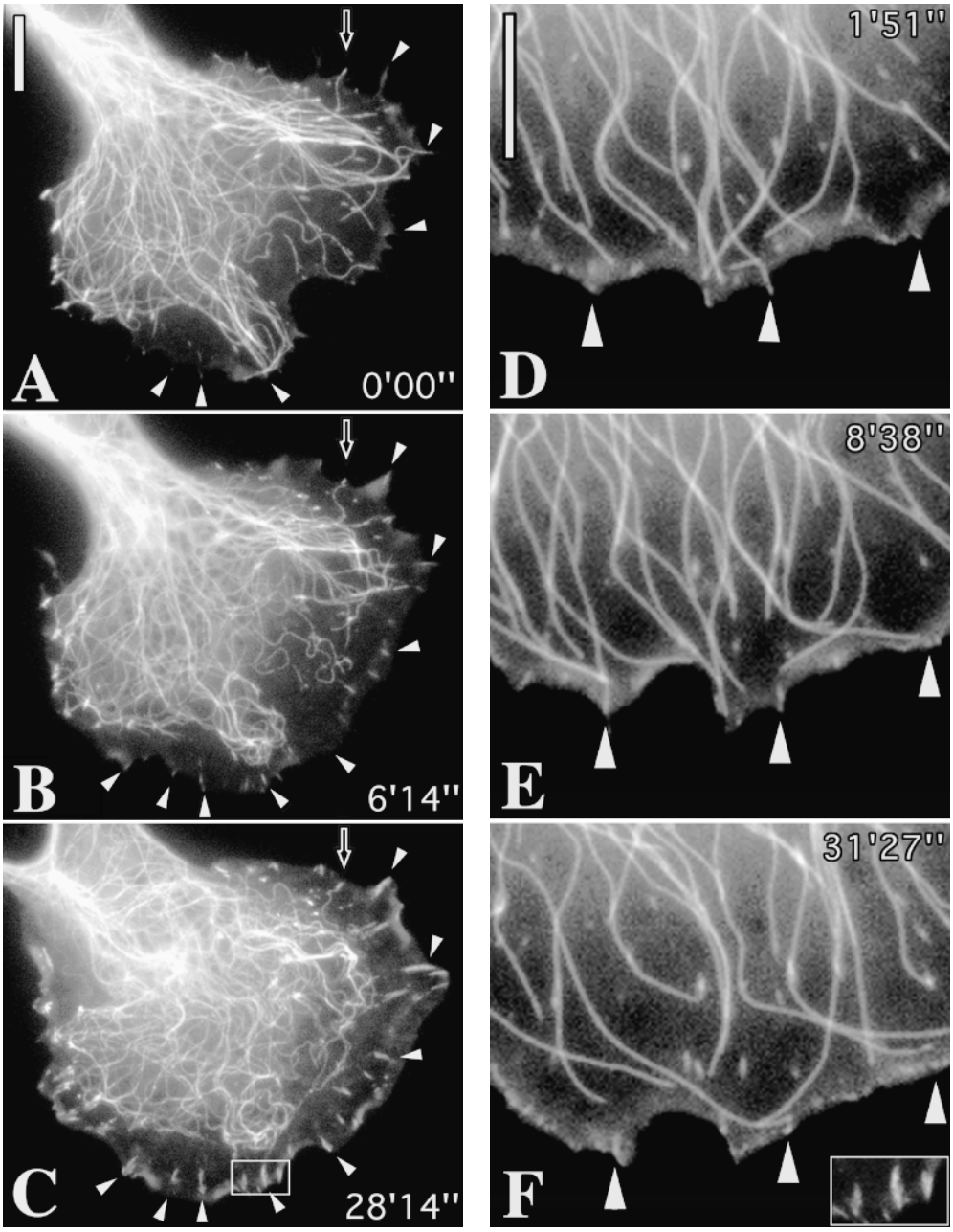

Figure 3. Elimination of targeting leads to contact growth. (A–C) Sequences of a cell coinjected with Rh-tubulin and Rh-vinculin and pretreated with 20 μM taxol for 30 min (A) to stabilize microtubules, before injection of L61 Rac at time 0:00. Arrowheads indicate peripheral contact sites that grew in the protruding cell edge induced by Rac. Hollow arrowhead indicates a contact that remained in association with a microtubule end and that did not grow. (D–F) control cell injected with Rac but not treated with taxol. Contact sites are targeted and do not enlarge. Bars, 10 μm. Videos available at http://www.jcb.org/cgi/content/full/146/5/1033/F3/DC1

we examined the effect of short term recovery of microtubules from depolymerization by nocodazole. This was most conveniently achieved through the temporal application of nocodazole (50 μg/ml) through a micro-pipette to one side of a cell. When locally applied for 15–20 min, nocodazole caused the depolymerization of peripheral microtubules in approximately one cell quadrant, adjacent to the needle tip (not shown). The phase of recovery was associated with either the retraction or protrusion of the cell edge and in both cases was accompanied by the dissolution of peripheral contact sites. A typical example of retraction (total of 5 cells examined: total of 80 contacts) is shown in Fig. 6. In this example, 8 peripheral contacts were targeted by individual microtubules that grew out to the cell periphery. Each targeting event was followed by a decrease in vinculin label in the contact, culminating with contact release and retraction of the cell edge.

Contacts Can Be Remodeled and Contact Groups Tailored by Targeting Microtubules

Two further aspects of contact targeting are shown in Fig. 7. In Fig. 7 A, the fate is shown of the medially situated contact outlined by a circle in Fig. 5. This contact, originally oriented in the direction of cell protrusion (single arrowhead, Fig. 7), was subsequently divided into two contacts oriented along the axis of the retracting cell edge. Division of the contact was associated with microtubule targeting from opposite directions (from below in the figure at 0′00″ and 3′40″ and from above at 4′46″ and 5′30″).

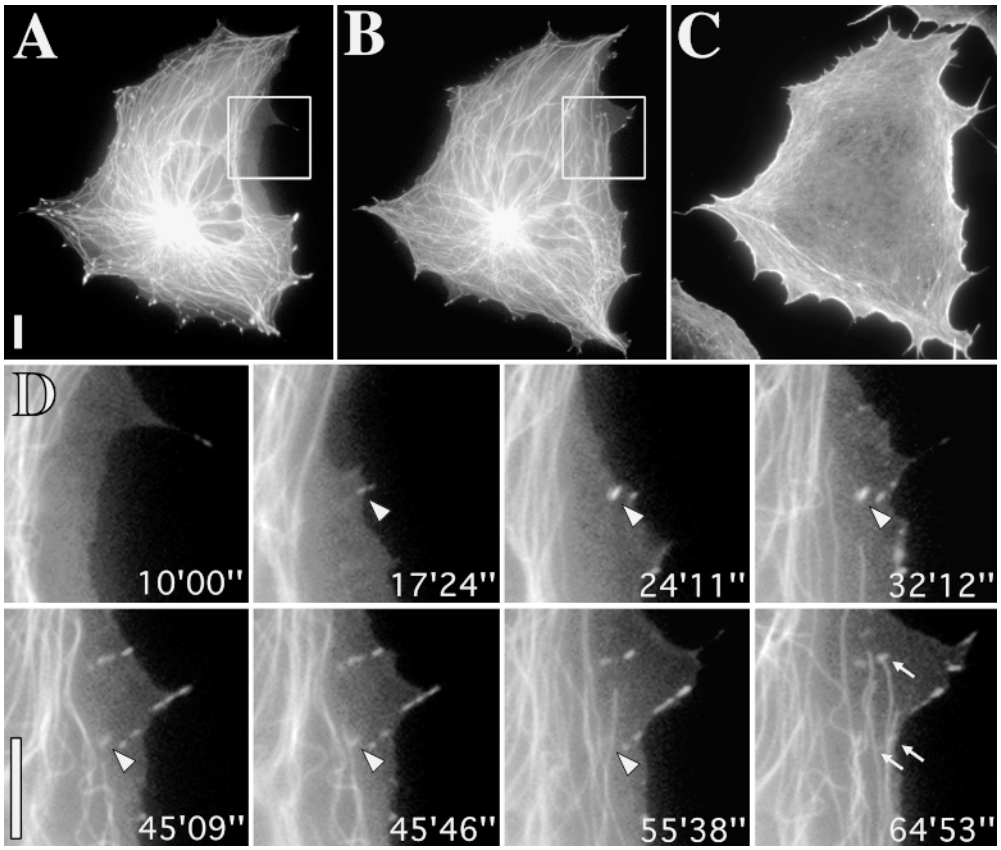

Figure 4. Rho-kinase independent contact sites are also targeted by microtubules. (A–C) low magnification view of cell incubated in 100 μM Y-27632. A and B correspond to the beginning and end of the sequence and C to the phalloidin-labeled image obtained after fixation immediately after the sequence. Cell was transiently cotransfected with tubulin-EGFP and zyxin-EGFP. D, video sequence of inset region in A and B showing targeting of newly formed contact sites. Zyxin-containing site marked with arrowhead, which appeared at time 17′24″ was targeted by a microtubule between 45′ and 46′ and had disappeared by 55′. Arrows indicate other sites that were targeted by microtubule ends. Bars, 10 μM. Videos available at http://www.jcb.org/cgi/content/full/146/5/1033/F4/DC1

11 similar remodeling events were observed in 7 other cells.

The spatially selective effect of targeting is likewise illustrated in the example shown in Fig. 7 B. Here, the fate of a closely packed group of contact sites is shown during microtubule recovery in a cell that had initially spread in the presence of nocodazole (as for Fig. 2). The cell was doubly transfected with EGFP-tagged tubulin and zyxin. During recovery, one of the contacts (position marked by arrowhead) disappeared from the group and this contact alone was targeted by microtubules, at times 3′42″ and 21′35″. The selective dissolution of contact sites after microtubule targeting during recovery from nocodazole was observed for 25 contacts in 11 cells.

Locally Applied Contractility Inhibitors Mimic Microtubule-mediated Cell Edge Retraction and Destabilize Microtubules

Since a link between microtubules and the tension developed by stress fiber bundles has already been suggested (see introduction), we considered that strain-dependent signals may play a role in the targeting process. If so, it was to be expected that the relaxation of tension by external means would affect microtubule-contact interactions. To test this presumption, relaxants of actomyosin contractility were applied locally to cells that had been preinjected with rhodamine-tagged tubulin and vinculin.

As antagonists, we used the myosin light chain kinase inhibitor, ML-7, and the myosin antagonist, BDM. Concentrations in the needle for local application were 2 mM for ML-7 and ~0.5 M (saturated), for BDM. Since each inhibitor gave essentially the same result, only one example, with ML-7, is shown (Fig. 8). In this figure the center of the ellipse corresponded to the point of application of the drug, with the needle directing the flow of inhibitor away from the cell edge. Two effects were observed. First, microtubules depolymerized from affected cell edge and this was followed by the release of contacts and their inward retraction. Outside the region of ML-7 influence (top of cell in Fig. 8), contact sites and microtubules were unaffected. The same result was obtained with a total of 5 cells treated with BDM (total of 157 contacts analyzed) and for 3 cells treated with ML-7 (total of 81 contacts analyzed).

In parallel experiments, we treated CAR cells on coverslips with 50 mM BDM, fixed them after different times, and performed immunolabeling for tubulin and vinculin. Under these conditions, microtubules shrank towards the cell center so that after 30 min only a remnant of the microtubule cytoskeleton remained around the centrosome.

Discussion

Based on the observation that microtubule ends invaded vinculin positive contact sites in fibroblast lamellipodia, we earlier speculated (Small and Rinnerthaler, 1985; Rinnerthaler et al., 1988) that microtubules act to stabilize or potentiate the growth of substrate adhesions. Our present findings indicate that quite the opposite is the case, namely that microtubules exert a negative influence on contact development. As we have recently demonstrated (Kaverina

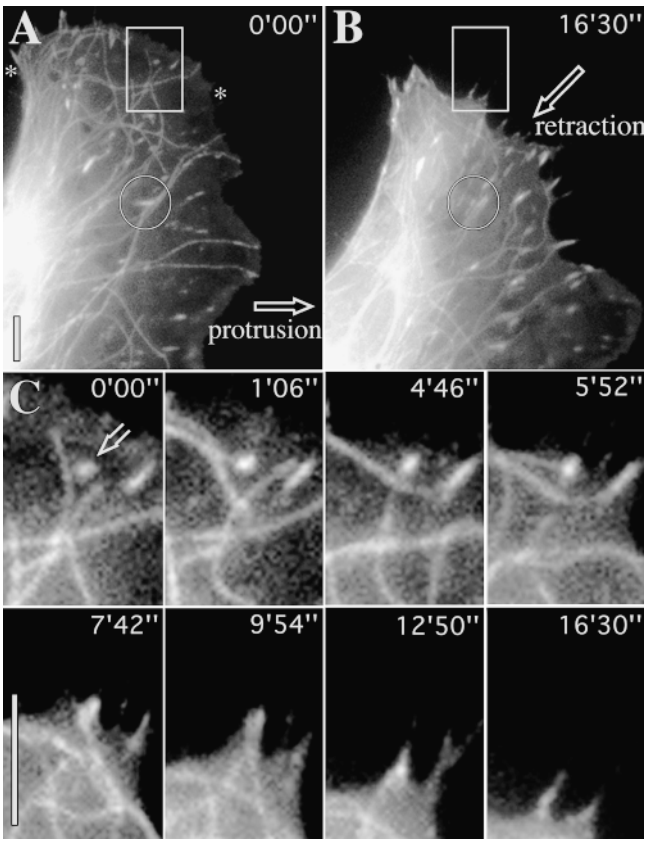

Figure 5. Repetitive targeting of peripheral focal adhesions precedes cell edge retraction. (A and B) First and last frames of a video sequence of a locomoting fish fibroblast that was coinjected with Rh-vinculin and Rh-tubulin. During the sequence, the region between the asterisks was retracted towards the cell body. (C) Video sequence of inset in A and B showing the typical fate of a contact site. Sequential frames show six targeting events at contact site (indicated by open arrow at 0′00″) by microtubules approaching from different directions. Inward retraction began after the 4th event. Circle in A indicates inset region shown in Fig. 7 A. Bars, 10 μM. Videos available at http://www.jcb.org/cgi/content/full/146/5/1033/F5/DC1

et al., 1998), the interaction of microtubules with contact sites is by no means fortuitous, but entails a direct engagement that can involve a modulation in microtubule dynamics. The present results show that microtubules, in a reciprocal manner, influence the development and turnover of substrate contact sites. We propose that by this route microtubules exert the influence on the actin cytoskeleton which underlies their control of cell polarization.

By virtue of their fibrillar nature and dynamic growth characteristics, microtubules are ideally suited for the point delivery of molecular complexes. Since contact formation is under the control of the small Rho-GTPases it is most likely that microtubules intervene in one or more of their signaling pathways. Indeed, in vitro experiments have already revealed the association with microtubules of a number of potential candidates that could be involved, including Rac (Best et al., 1996), the Rac/Rho GEFs, H1 (Ren et al., 1998), and Vav (Fernandez et al., 1999), as well as the oncoprotein Lfc (Glaven et al., 1999). Since only the immediate proximity of microtubules affects the development of contact sites, we presume that the effectors responsible for modulation are specifically concentrated at microtubule ends. In yeast, the accumulation or acquisition of molecular assemblies at the ends of microtubules is evident during mitosis (Saunders, 1999) and the concentration of tea1 at the ends of interphase microtubules appears to play a role in the determination of cell polarity (Mata and Nurse, 1997). Further, in vertebrate fibroblasts, CLIP-170, whose *Drosophila* homologue binds myosin VI (Lantz and Miller, 1998), accumulates at the growing, but not at the shrinking ends of microtubules (Perez et al., 1999). Regulatory factors could be delivered to the end of microtubules by molecular motors, one possible candidate being the Rac and Cdc42 effector MLK2, which associates with KIF3 kinesin (Nagata et al., 1998).

A primary conclusion from this study is that factors concentrated at the ends of microtubules are brought by microtubule growth into the proximity of substrate contacts to influence their development, by modulating acto-myosin contractility. Acto-myosin–based contractility, stimulated via phosphorylation of the myosin II regulatory light chain, has been shown necessary for the formation of stress fiber bundles and focal adhesions (reviewed in Schoenwalder and Burridge, 1999). Accordingly, inhibitors of contractility, such as BDM, or of myosin light chain kinase, cause the dissociation of focal adhesions, or block their formation in response to the upregulation of Rho (Chrzanowska and Burridge, 1996). Other studies (reviewed in Narumiya et al., 1997) have shown that the Rho-associated kinase, p160ROCK or Rho-kinase, acts downstream of Rho and stimulates myosin phosphorylation by inhibiting the myosin light chain phosphatase. At the same time, it has become apparent that not all substrate contact sites depend on Rho-kinase for their formation. In particular, peripheral contact assemblies similar to focal complexes induced by Rac (Nobes and Hall, 1995) are formed in cells in which Rho-kinase is specifically inhibited (Uehata et al., 1997; Rottner et al., 1999). Despite their independence of Rho-kinase, these contact sites are likewise dissociated by both BDM and ML-7 (Rottner et al., 1999) and therefore also depend on myosin II–based contractility for their maintenance. Thus, the development of Rho-kinase–independent contacts, which serve to support the protrusive activity of the cell front (Rottner et al., 1999) may also be regulated via modulations in contractility.

Since targeting events correlated with the diminution, retraction, or dissociation of contact sites, it is evident that microtubule targeting serves to antagonize contact development. This was supported by our finding that a block in targeting activity caused the uncontrolled growth of peripheral contacts. Former studies (Danowski, 1989; Bershadsky et al., 1996) have linked microtubule disassembly with the enhancement of contractility. We propose that a converse mechanism exists whereby the targeted growth of microtubules into contact sites mediates a highly localized relaxation and that this is the mechanism by which contact growth is reversed or retarded. Consistent with this conclusion was the finding that intensive targeting of contacts at cell edges and the application of myosin inhibitors produced similar effects.

As we have seen, the retraction of an adhesion site at a

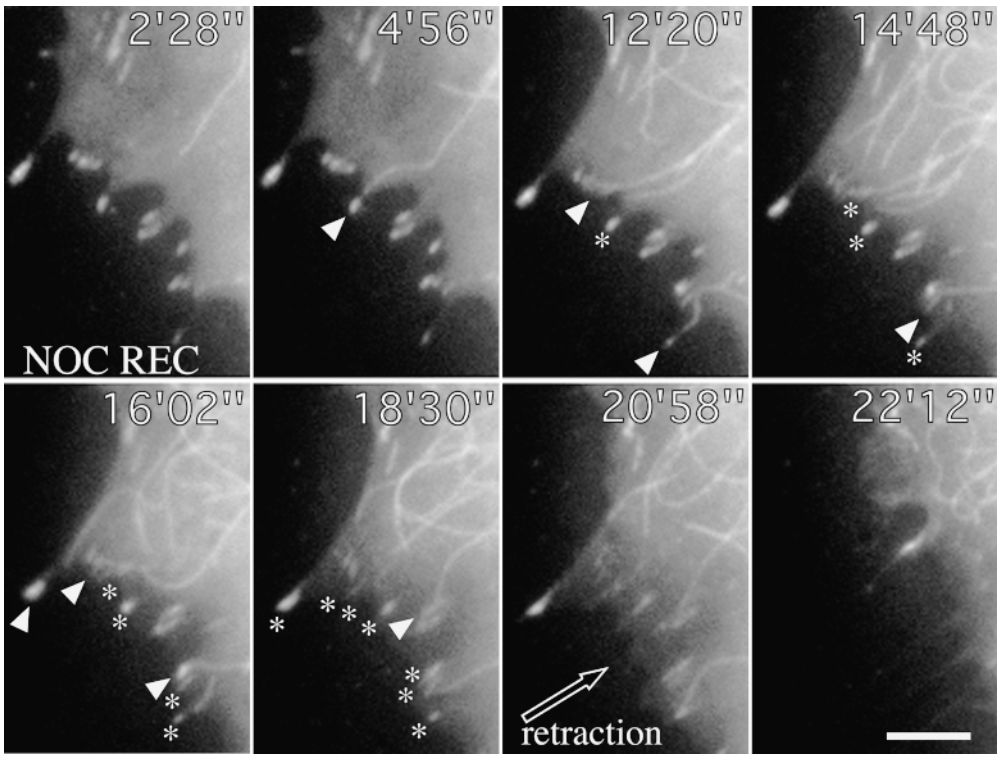

Figure 6. Contact targeting and retraction after recovery from local application of nocodazole. Cell shown was cotransfected with zyxin-EGFP and tubulin-EGFP and treated on one edge with 50 μg/ml nocodazole applied through a microneedle to locally depolymerize microtubules. Video sequences show recovery after removal of needle at time 0′00″. Arrowheads indicate sequential targeting events at peripheral contact sites and asterisks the positions of contacts that had already been targeted. Time is in minutes and seconds. Bar, 5 μM. Video available at http://www.jcb.org/cgi/content/full/146/5/1033/F6/DC1

trailing cell edge may be preceded by multiple targeting events. These findings are generally supported by the statistical characterization of regional microtubule dynamics by Wadsworth (1999); her studies showed that microtubule ends close to nonmotile edges exhibited shorter excursions and frequent catastrophes, whereas longer excursions and fewer catastrophes occurred in protruding regions. The shorter and more frequent excursions would correspond to what we observe at cell edges destined for retraction. We conclude that a single targeting event serves to provide a quantum relaxation dose and that further doses, as required, must be supplied by freshly

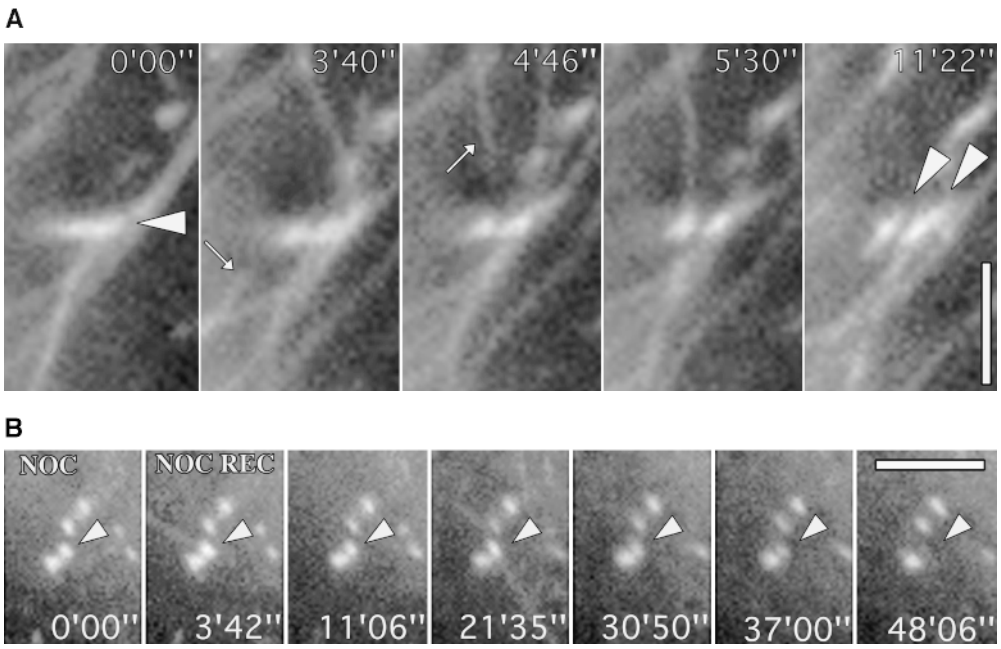

Figure 7. (A) Contact site remodeling. A shows video sequence of medial focal adhesion outlined by a circle in Fig. 5, A and B. This contact site was targeted by microtubules from below and above (approaching microtubules are indicated by arrows at 3′40″ and 4′46″), and then split into two contacts oriented at around 45° to the parent contact (see arrowheads at 0′00″ and 11′22″). (B) Tailoring of contact group. B shows video sequence of a group of contacts in a cell cotransfected with zyxin-EGFP and tubulin-EGFP during recovery from nocodazole. The second contact from bottom was selectively targeted by microtubules at 3′42″ and 21′35″ and had disappeared at 48′. Bars: (A) 3 μM; (B) 5 μM. Videos available at http://www.jcb.org/cgi/content/full/146/5/1033/F7/DC1

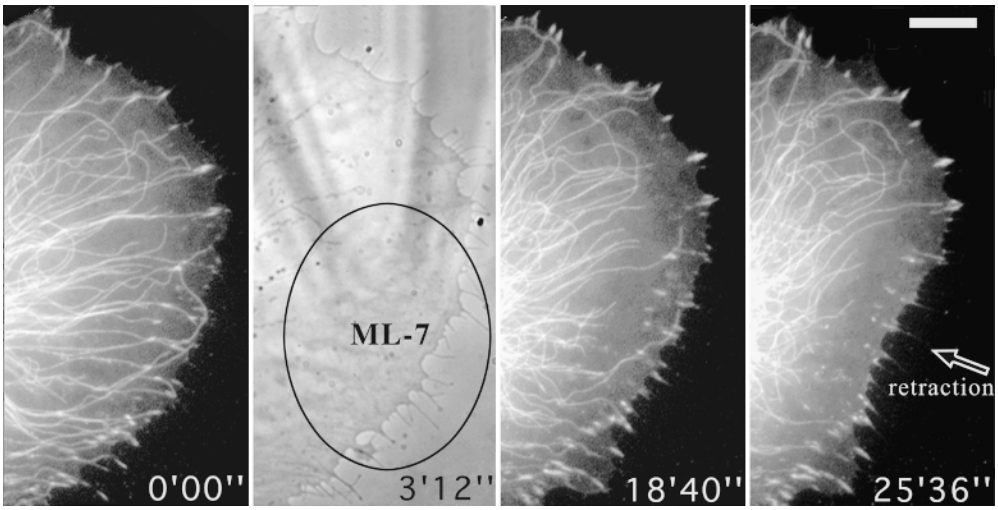

Figure 8. Locally applied ML-7 destabilizes microtubules and induces the dissociation of peripheral contact sites. Figure shows video sequence of a cell cotransfected with zyxin-EGFP and tubulin-EGFP that was treated topically, from time 0′00″ with a local application of 2 mM ML-7 through a microneedle (visible in the phase contrast image at 3′12″), over the region indicated by the ellipse. Bar, 10 μM. Video available at http://www.jcb.org/cgi/content/full/146/5/1033/F8/DC1

charged microtubule ends in subsequent targeting forays. By modulating the number of targeting events, differential relaxation effects may then be exerted on contact assemblies in different regions of a cell. In this way, microtubule signaling at contact sites could modulate the substrate contact pattern of a cell and thereby determine its polarity (Fig. 9).

In a recent study, Pelham and Wang (1999) provided the most detailed tension patterns yet of a locomoting fibroblast. Their results show a high, but fluctuating level of tension at the cell front and a lower but constant tension in the trailing cell rear. It is further proposed that mechanical forces play an important role in signal transduction. In this context, we suggest that microtubules are important players in these signal transduction events. In response to tension-sensing cues propagated through the actin cytoskeleton, microtubules could be guided to contact sites to control tension according to the requirements for protrusion or retraction. Indeed, the rapid depolymerization of microtubules in response to the treatment of cells with contractility inhibitors may reflect a general dependence of microtubule stability on a stressed actin cytoskeleton. It is noteworthy that the microtubule destabilizing effect we observed with myosin inhibitors was not detected in previous studies (Lin et al., 1996; Waterman-Storer and Salmon, 1997). This can be explained for BDM by the use here of both higher concentrations and longer times; a higher sensitivity of CAR cells to BDM can also not be excluded. That the effect was not simply an artefact induced by high concentrations of BDM is suggested by the obser-

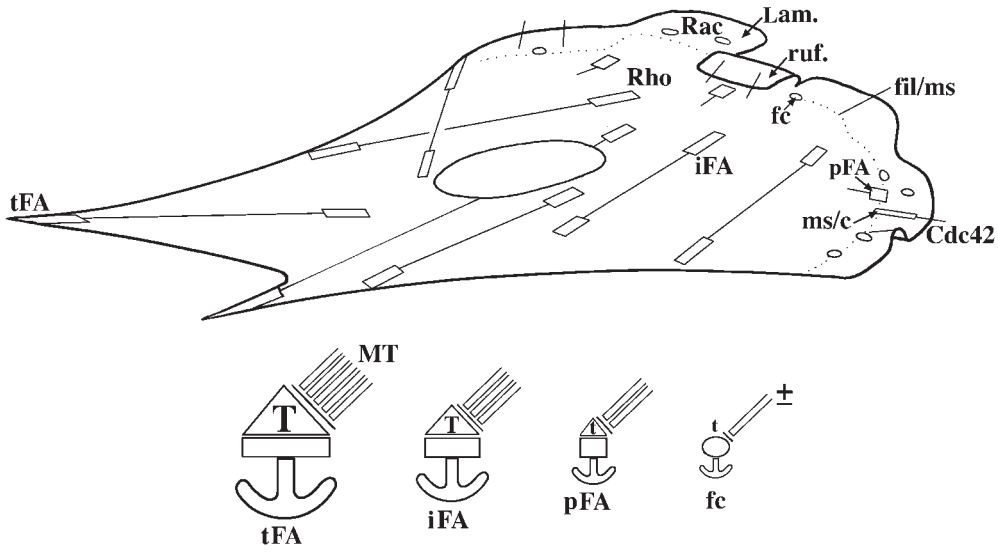

Figure 9. Schematic illustration of substrate contact dynamics in a moving fibroblast. (Top) Substrate contacts are initiated in the protruding and ruffling lamellipodium (Lam, ruf). Two classes of primary contacts are depicted: punctate focal complexes (fc) and linear contacts associated with some microspike bundles (ms/c). Their formation is associated with the activation of Rac and Cdc42, respectively. Each type of primary contact can develop into a precursor of a focal adhesion (pFA). Further abbreviations: iFA, intermediate focal adhesion in the body of the cell; tFA, focal adhesion at a trailing cell edge. (Bottom) Four types of contact sites with different strengths of anchorage to the substrate (anchors) are depicted and correspond to those in the upper diagram. All sites rely on contractility for their maintenance, indicated by different levels of myosin II–dependent tension (T and t). For precursor (pFA) and mature focal adhesions (iFA, tFA), myosin activation depends on Rho-kinase. The contractility of focal complexes is Rho-kinase independent. Microtubules (MT) interface with contact sites and modulate their turnover by locally inhibiting contractility. The relaxing dose is controlled by the total number and frequency of microtubule targeting events. Focal complexes may or may not be targeted by microtubules.

vation that the myosin light chain kinase inhibitor, ML-7, produced the same result. Chrzanowska and Burridge (1996) showed that the alternative inhibitor, H-7, applied at a concentration of 300 μM for 30 min dissociates focal adhesions in REF-52 fibroblasts; under these same conditions, we also observed microtubule destabilization, culminating in the shrinkage of the microtubule cytoskeleton to the perinuclear area (not shown). In line with our own studies, Cook et al. (1998) found that elevated levels of Rho, which increases contractility, lead to a stabilization of microtubules.

An alternative view of the way microtubules may determine cell polarity has been put forward by Waterman-Storer et al. (1999), who showed that the polymerization of microtubules during the recovery of Swiss 3T3 cells from nocodazole was associated with the upregulation of Rac and the corresponding induction of membrane ruffling. They suggested that this effect may be explained by the generation of Rac-GTP at microtubule ends. Such a mechanism was, however, difficult to reconcile with the continued elevation of Rac-GTP long after microtubule polymerization was complete (Waterman-Storer et al., 1999). As in earlier studies (Bershadsky and Vasiliev, 1988; Rinnerthaler et al., 1988; Sammak and Borisy, 1988), these authors noted a penetration of microtubules into regions of active protrusion and further noted a correlation between protrusive activity and dynamic microtubule growth, rather than with polymer mass. However, protruding cell edges in rapidly motile cells can have very few associated microtubules (Euteneuer and Schliwa, 1984; Wadsworth, 1999; our unpublished observations), making it unlikely that active Rac is generated from microtubule ends at the cell front. An alternative explanation of their result is provided by the finding that Rac and Rho antagonize each others activities (Kozma et al., 1997; van Leeuwen et al., 1997; Hirose et al., 1998; Moorman et al., 1999; Rottner et al., 1999). As has previously been demonstrated, microtubule depolymerization leads to the upregulation of Rho (Bershadsky et al., 1996; Enomoto, 1996) and microtubule polymerization to its downregulation, reflected here in the dissolution of focal adhesions during recovery from nocodazole. We surmise that the upregulation of Rac observed during microtubule polymerization (Waterman-Storer et al., 1999) is an indirect result of the downregulation of Rho (Rottner et al., 1999) and not to the microtubule-dependent generation of Rac at the cell front.

Further work will be required to demonstrate the means of guidance of microtubules to contact sites and the nature of the relaxing signal they convey to regulate contact dynamics. As regards the signal, since both Rho-kinase–dependent focal adhesions and Rho-kinase–independent focal complexes are modulated by microtubule targeting, we conclude that the point of intervention of microtubule-bound modulators in the pathway leading to contractility is downstream of Rho-kinase.

The authors thank Drs. T. Hyman, R. Tournebize, J. Peloquin, and G. Borisy for generous gifts of rhodamine tubulin and Cy-3 tubulin; Professor J. Wehland for the EGFP constructs for zyxin and tubulin; Drs. M. Gimona and K. Rottner for rhodamine vinculin and Professor H. Faulstich for Cy-3 Phalloidin. We also thank Ms. M. Schmittner and Ms. U. Mueller for technical and photographic assistance, Ms. E. Eppacher for manuscript processing and other members of the department for help, encouragement, and discussion. The Rho-kinase inhibitor Y27632 was kindly donated by Yoshitomi Pharmaceutical Industries Ltd. Japan.

The microscope systems used were funded in part from grants obtained from the Austrian Science Research Council, The Austrian National Bank and the Seegen Stiftung of the Austrian Academy of Sciences.

Submitted: 27 April 1999
Revised: 12 July 1999
Accepted: 15 July 1999

References

Bershadsky, A.D., and J.M. Vasiliev. 1988. Cytoskeleton. Plenum Press, New York. 298 pp.

Bershadsky, A., A. Chausovsky, E. Becker, A. Lyubimova, and B. Geiger. 1996. Involvement of microtubules in the control of adhesion-dependent signal transduction. *Curr. Biol.* 6:1279–1289.

Best, A., S. Ahmed, R. Kozma, and L. Lim. 1996. The Ras-related GTPase Rac1 binds tubulin. *J. Biol. Chem.* 271:3756–3762.

Chen, W.-T. 1981. Surface changes during retraction-induced spreading of fibroblasts. *J. Cell Sci.* 49:1–13.

Chrzanowska-Wodnicka, M., and K. Burridge. 1996. Rho-stimulated contractility drives the formation of stress fibers and focal adhesions. *J. Cell Biol.* 133: 1403–1415.

Cook, T.A., T. Nagasaki, and G.G. Gundersen. 1998. Rho guanosine triphosphatase mediates the selective stabilization of microtubules induced by lysophosphatidic acid. *J. Cell Biol.* 141:75–85.

Danowski, B.A. 1989. Fibroblast contractility and actin organization are stimulated by microtubule inhibitors. *J. Cell Sci.* 93:255–266.

Enomoto, T. 1996. Microtubule disruption induces the formation of actin stress fibers and focal adhesions in cultured cells: possible involvement of the Rho signal cascade. *Cell Struct. Funct.* 21:317–326.

Euteneuer, U., and M. Schliwa. 1984. Persistent, directional motility of cells and cytoplasmic fragments in the absence of microtubules. *Nature.* 310:58–61.

Fernandez, J.A., L.M. Keshvara, J.D. Peters, M.T. Furlong, M.L. Harrison, and R.L. Geahlen. 1999. Phosphorylation- and activation-independent association of the tyrosine kinase Syk and the tyrosine kinase substrates Cbl and Vav with tubulin in B-cells. *J. Biol. Chem.* 274:1401–1406.

Glaven, J.A., I. Whitehead, S. Bagrodia, R. Kay, and R.A. Cerione. 1999. The Dbl-related protein, Lfc, localizes to microtubules and mediates the activation of Rac signaling pathways in cells. *J. Biol. Chem.* 274:2279–2285.

Hirose, M., T. Ishizaki, N. Watanabe, M. Uehata, O. Kranenburg, W.H. Moolenaar, F. Matsumura, M. Maekawa, H. Bito, and S. Narumiya. 1998. Molecular dissection of the Rho-associated protein kinase (p160ROCK)-regulated neurite remodeling in neuroblastoma N1E-115 cells. *J. Cell Biol.* 41:1625–1636.

Kaverina, I., K. Rottner, and J.V. Small. 1998. Targeting, capture, and stabilization of microtubules at early focal adhesions. *J. Cell Biol.* 142:181–190.

Kozma, R., S. Sarner, S. Ahmed, and L. Lim. 1997. Rho family GTPases and neuronal growth cone remodeling: relationship between increased complexity induced by Cdc42Hs, Rac1, and acetylcholine and collapse induced by RhoA and lysophosphatidic acid. *Mol. Cell Biol.* 17:1201–1211.

Lantz, V.A., and K.G. Miller. 1998. A class VI unconventional myosin is associated with a homologue of a microtubule-binding protein, cytoplasmic linker protein-170, in neurons and at the posterior pole of *Drosophila* embryos. *J. Cell Biol.* 140:897–910.

Lin, C.H., E.M. Espreafico, M.S. Mooseker, and P. Forscher. Myosin drives retrograde F-actin flow in neuronal growth cones. *Neuron.* 16:769–782.

Mata, J., and P. Nurse. 1997. Tea1 and the micromanipulator cytoskeleton are important for generating global spatial order within the fission yeast cell. *Cell.* 89:939–949.

Moorman, J.P., D. Luu, J. Wickham, D.A. Bobak, and C.S. Hahn. 1999. A balance of signaling by Rho family small GTPases RhoA, Rac1 and Cdc42 coordinates cytoskeletal morphology but no cell survival. *Oncogene.* 18:47–57.

Nagata, K., A. Puls, C. Futter, P. Aspenstrom, E. Schaefer, T. Nakata, N. Hirokawa, and A. Hall. 1998. The MAP kinase kinase kinase MLK2 co-localizes with activated JNK along microtubules and associates with kinesin superfamily motor KIF3. *EMBO (Eur. Mol. Biol. Organ.) J.* 17:149–158.

Narumiya, S., T. Ishizaki, and N. Watanabe. 1997. Rho effectors and reorganization of actin cytoskeleton. *FEBS Lett.* 410:68–72.

Nobes, C.D., and A. Hall. 1995. Rho, Rac, and Cdc42 GTPases regulate the assembly of multimolecular focal complexes associated with actin stress fibers, lamellipodia, and filopodia. *Cell.* 81:53–62.

Pelham, R.J., Jr., and Y.-L. Wang. 1999. High resolution detection of mechanical forces exerted by locomoting fibroblasts on the substrate. *Mol. Biol. Cell.* 10:935–945.

Perez, F., G.S. Diamantopoulos, R. Stalder, and T.E. Kreis. 1999. CLIP-170 highlights growing microtubule ends in vivo. *Cell.* 96:517–527.

Ren, Y., R. Li, Y. Zheng, and H. Busch. 1998. Cloning and characterization of GEF-H1, a microtubule-associated guanine nucleotide exchange factor for Rac and Rho GTPases. *J. Biol. Chem.* 273:34954–34960.

Rinnerthaler, G., B. Geiger, and J.V. Small. 1988. Contact formation during fibroblast locomotion: involvement of membrane ruffles and microtubules. *J. Cell Biol.* 106:747–760.

Rottner, K., A. Hall, and J.V. Small. 1999. Interplay between Rac and Rho in the control of substrate contact dynamics. *Curr. Biol.* 9:640–648.

Sammak, P.J., and G.G. Borisy. 1988. Direct observation of microtubule dynamics in living cells. *Nature.* 332:724–726.

Saunders, W.S. 1999. Action at the ends of microtubules. *Curr. Opin. Cell Biol.* 11:129–133.

Schoenwaelder, S.M., and K. Burridge. 1999. Bidirectional signaling between the cytoskeleton and integrins. *Curr. Opin. Cell Biol.* 11:274–286.

Small, J.V., and G. Rinnerthaler. 1985. Cytostructural dynamics of contact formation during fibroblast locomotion in vitro. *Exp. Biol. Med.* 10:54–68.

Uehata, M., T. Ishizaki, H. Satoh, T. Ono, T. Kawahara, T. Mosirshita, H. Tamakawa, K. Yamagami, J. Inui, M. Maekawa, and S. Narumiya. 1997. Calcium sensitization of smooth muscle mediated by a Rho-associated protein kinase in hypertension. *Nature.* 389:990–994.

Van Leeuwen, F.N., H.E.T. Kain, R.A. Van der Kammen, F. Michiels, O.W. Kranenburg, and J.G. Collard. 1997. The guanine nucleotide exchange factor Tiam 1 affects neuronal morphology; opposing roles for the small GTPases Rac and Rho. *J. Cell Biol.* 139:797–807.

Vasiliev, J.M., and I.M. Gelfand. 1976. Effects of colcemid on morphogenetic processes and locomotion of fibroblasts. *In* Cell Motility. Cold Spring Harbor Laboratory Press, Cold Spring Harbor, NY. 279–304.

Wadsworth, P. 1999. Regional regulation of microtubule dynamics in polarized, motile cells. *Cell Motil. Cytoskel.* 42:48–59.

Waterman-Storer, C.M., and E.D. Salmon. 1997. Actomyosin-based retrograde flow of microtubules in the lamella of migrating epithelial cells influences microtubule dynamic instability and turnover and is associated with microtubule breakage and treadmilling. *J. Cell Biol.* 139:417–434.

Waterman-Storer, C.M., R.A. Worthylake, B.P. Liu, K. Burridge, and E.D. Salmon. 1999. Microtubule growth activates Rac1 to promote lamellipodial protrusion in fibroblasts. *Nature Cell Biol.* 1:45–50.